The dielectric dispersion of liquid-filled porous sintered materials

The dielectric dispersion of liquid-filled porous sintered materials

B Nettelblad† and G A Niklasson‡

† Physics Department, Chalmers University of Technology, S-412 96 Göteborg, Sweden
‡ Teknikum, Uppsala University, Box 534, S-751 21 Uppsala, Sweden

Abstract. We have used a differential effective-medium (DEM) theory to model the dielectric properties of sintered glass beads, impregnated with salty water, in the kHz and MHz ranges. The starting point of the theory is a lattice of touching spheres in pore liquid. The sintering is modelled by adding solid material and using the DEM method to calculate the dielectric response. Dipolar interactions in the system are treated by using effective depolarization factors, obtained from the dependence of the formation factor on porosity. The frequency dependence of the formation factor is in good agreement with experimental data. For the real part of the dielectric permittivity, discrepancies arise at low frequencies. This is probably due to percolation effects.

1. Introduction

The dielectric properties of liquid-impregnated porous solids are of interest in several applications. For example, sedimentary rocks can contain crude oil and natural gas as well as water. In such cases, dielectric measurements can be used for oil exploration [1]. In electrical insulation systems, oil-impregnated paper is prevalent, and the interest in the electric properties of such systems is obvious. Building materials, such as cement, constitute another type of porous material. Here, excessive amounts of pore water can severely impair the mechanical properties of the material. It has been proposed that measurements of the dielectric response can be used for nondestructive testing of cement [2].

In spite of considerable theoretical and experimental efforts, the dielectric properties of porous materials are still quite poorly understood. In several cases, model systems of so-called artificial rocks have been studied. One type of artificial rock is materials made of sintered grains, i.e., the specimens are heated, causing the grains to fuse. We have previously shown [3] that a material consisting of sintered polypropylene beads possesses some similarities with materials consisting of sintered glass spheres, as far as the electrical properties are concerned.

In this paper, we consider the dielectric spectrum in the kHz to MHz range of brine-filled materials consisting of sintered glass beads. A model proposed by Sheng [4, 5] and by Schwartz [6] is extended to frequency-dependent properties to describe the spectrum and its dependence on porosity. We consider the sample processing to have two stages: initially, a packing of the spheres; and secondly, the sintering process, which is modelled as a cementation.

Table 1. Data on Archie's law parameters obtained previously for different systems of impregnated porous sintered solids.

Reference	Type of material	a	m
Wong *et al* [8]	Monosize spherical glass beads	3.3	2.3
Holwech and Nøst [9]	Monosize spherical glass beads	3.0	2.2
Nøst *et al* [10]	Monosize spherical glass beads	4.8	2.5
Brouers and Ramsamugh [11]	Alumina ceramics (initial grain appearance unknown)	1.1	1.9
Nettelblad [3]	Multisize nonspherical polypropylene beads	1.7	2.4
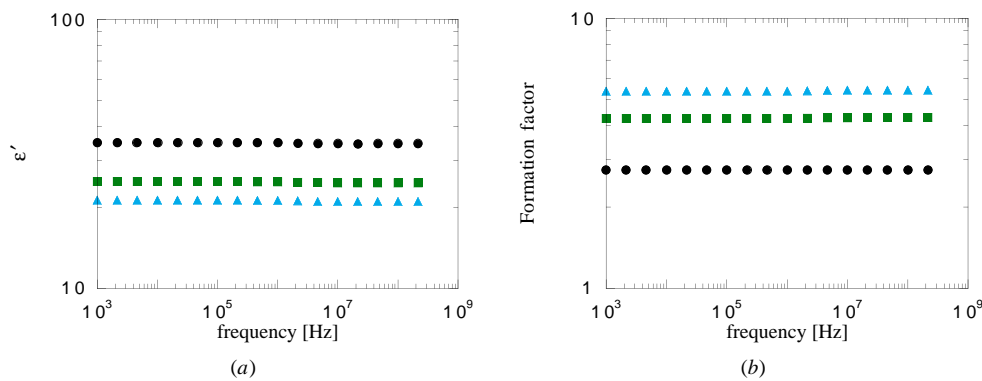
Figure 1. The permittivities (*a*) and formation factors (*b*) of s.c. lattices (circles), b.c.c. lattices (squares) and f.c.c. lattices (triangles) of touching spheres, calculated using the grain consolidation model. Note that the porosities are different for the different lattices.

2. Theoretical background

For brine-saturated porous rocks, Archie [7] found an empirical relation that is widely known as Archie's law:

$$\sigma_{app} = \sigma_f a \varphi^m. \tag{1}$$

Here, σ_{app} is the apparent conductivity of the rock, σ_f the conductivity of the fluid and φ the porosity, i.e., the volume fraction of pores. Originally, it was assumed that $a = 1$, but it was later found that this had to be modified. For impregnated porous samples made of sintered materials (for example sintered glass beads impregnated with salty water) values of a different from unity have been obtained, as is shown in table 1, together with values of m. A commonly used concept is the formation factor, defined as σ_f/σ_{app} (assuming a proportional dependence without contributions from interface conduction). Different effective-medium theories on the dielectric properties of composite materials can be obtained by making different assumptions about the microstructure. They are in principle valid for all solid volume fractions, but restrictions may occur in practice. For example, the model of Maxwell Garnett [12] assumes that one of the phases (generally the solid) forms inclusions within the other phase. For spherical solid inclusions in the fluid this model yields for the

complex permittivity

$$\frac{\varepsilon_{app} - \varepsilon_f}{\varepsilon_{app} + 2\varepsilon_f} = v_s \frac{\varepsilon_s - \varepsilon_f}{\varepsilon_s + 2\varepsilon_f}. \tag{2}$$

Here, ε_{app} is the apparent permittivity of the composite material, ε_f and ε_s are the permittivities of the fluid and the solid respectively, and v_s is the volume fraction of the solid (note that $v_s = 1 - \varphi$). For insulating inclusions in a conducting medium, this equation yields for the apparent conductivity

$$\sigma_{app} = \sigma_f \frac{2\varphi}{3 - \varphi}. \tag{3}$$

The symmetric model of Bruggeman [13] yields the following equations:

$$\varphi \frac{\varepsilon_f - \varepsilon_{app}}{\varepsilon_f + 2\varepsilon_{app}} + v_s \frac{\varepsilon_s - \varepsilon_{app}}{\varepsilon_s + 2\varepsilon_{app}} = 0 \tag{4}$$

$$\sigma_{app} = \sigma_f \frac{3\varphi - 1}{2} \qquad \left(\varphi \geqslant \tfrac{1}{3}\right). \tag{5}$$

Note that these models are not able to reproduce equation (1). Another type of effective-medium theory are integration methods or differential effective-medium theory. In such methods, one starts with the pure host material, and adds infinitesimal amounts of guest material in several stages. For each addition, one uses the Maxwell Garnett formula for dilute suspensions to calculate σ_{app}—however, with σ_f determined by a similar calculation at the previous stage. Integration then yields

$$\frac{\varepsilon_s - \varepsilon_{app}}{\varepsilon_s - \varepsilon_f} = \varphi \left(\frac{\varepsilon_{app}}{\varepsilon_f}\right)^{1/3} \tag{6}$$

which for spherical insulating inclusions in a conducting medium becomes

$$\sigma_{app} = \sigma_f \varphi^{1.5}. \tag{7}$$

Other exponents are obtained if, e.g., ellipsoids are used. For fully aligned ellipsoids, it has been shown that [14, 15]

$$\frac{\varepsilon_s - \varepsilon_{app}}{\varepsilon_s - \varepsilon_f} = \varphi \left(\frac{\varepsilon_{app}}{\varepsilon_f}\right)^{A_k} \tag{8}$$

and

$$\sigma_{app} = \sigma_f \varphi^{1/(1 - A_k)} \tag{9}$$

where the depolarization factor, A_k, follows from

$$A_k = \frac{x_1 x_2 x_3}{2} \int_0^\infty \frac{\mathrm{d}u}{\left(x_k^2 + u\right) \left[\left(x_1^2 + u\right) \left(x_2^2 + u\right) \left(x_3^2 + u\right)\right]^{1/2}} \tag{10}$$

where x_1, x_2 and x_3 are the semi-axes of the ellipsoid.

For randomly oriented ellipsoids, the corresponding result is [15, 16]

$$\varphi = \left(\frac{\varepsilon_f}{\varepsilon_{app}}\right)^{3d} \left(\frac{\varepsilon_s - \varepsilon_{app}}{\varepsilon_s - \varepsilon_f}\right) \left(\frac{\varepsilon_f - r\varepsilon_s}{\varepsilon_{app} - r\varepsilon_s}\right)^R \left(\frac{\varepsilon_f - q\varepsilon_s}{\varepsilon_{app} - q\varepsilon_s}\right)^Q \tag{11}$$

where

$$d = (1/A_1 + 1/A_2 + 1/A_3)^{-1}$$
$$k = A_1 A_2 + A_1 A_3 + A_2 A_3$$
$$q = -\frac{1 - k - (1 - 3k)^{0.5}}{1 + k}$$
$$r = -\frac{1 - k + (1 - 3k)^{0.5}}{1 + k} \tag{12}$$
$$Q = \frac{(1 - 2k - 3d)q + 2(k - 3d)}{2(1 - 3k)^{0.5}}$$
$$R = \frac{(1 - 2k - 3d)r + 2(k - 3d)}{2(1 - 3k)^{0.5}}.$$

For nonconducting inclusions in an electrolyte, we obtain

$$\sigma_{app} - \sigma_f \varphi^{1/(1-3d-R-Q)}. \tag{13}$$

This technique is thus able to reproduce Archie's law with the prefactor $a = 1$, and with various values of the exponent m. The exponent is thus dependent on the shape of the particles. It should be mentioned that the exponent 1.5 obtained for spheres is a minimum for randomly oriented particles, and going to nonspherical inclusions will accordingly increase the value of the exponent.

Interestingly, the values of m obtained for sintered materials are very similar, as is shown in table 1. It appears as if the sintering process should yield an Archie-like behaviour with an exponent in the range 2.0–2.5, probably dependent on the exact processing procedure.

Still, equations (9) and (13) are not able to reproduce a prefactor $a \neq 1$. Sheng [4, 5] was able to obtain a prefactor different from one, in an analogous three-component theory. In an elaboration of this work, Schwartz [6] considered an initially unconsolidated mixture of solid and liquid (where the solid particles may be touching, making the composite bicontinuous). To this mixture, we add solid material in infinitesimal amounts until the desired volume fraction of solid is attained. The results when this approach is used differ from equations (8) and (11) in the respect that ε_f is altered to $\varepsilon_{initial}$, the dielectric constant of the initial mixture, and φ is altered to φ/φ_0, where φ_0 is the porosity of the initial mixture. The same applies to equations (9) and (13); equation (13) then becomes

$$\sigma_{app} = \frac{\sigma_f}{F_0} \left(\frac{\varphi}{\varphi_0} \right)^{1/(1-3d-R-Q)} \tag{14}$$

where F_0 is the formation factor of the initial mixture (an analogous expression is obtained instead of equation (9)). This means that we obtain a prefactor that can be different from unity. Sheng and Schwartz considered only the DC conductivity of the composite material. Yet, the principle of using an integration theory starting with an unconsolidated pack, whose properties can be estimated, is easily extended for calculating the frequency-dependent properties.

Holwech and Nøst gave data for the dielectric spectrum of samples consisting of sintered glass beads. They interpreted the results according to the spectral theory of Bergman [17] and Milton [18], and obtained Bergman–Milton spectra for their different samples. Such spectra may be useful in certain circumstances (they can be used to predict the effect of an exchange of pore liquid), but there is no clear explanation of why a certain spectrum is obtained. If our effective-medium method is able to reproduce measured data satisfactorily, it also gives an indication of why particular spectra are obtained.

Another model for calculating the dielectric spectrum of a porous solid was proposed by Hilfer [19]. Since the composite material is disordered, the porosity is varying on the meso-scale, and it is thus possible to define a local porosity distribution. To estimate the properties of the composite, a local percolation probability is postulated. Haslund *et al* [20] obtained good agreement between the predictions of theory and experiments. The local porosity distribution was obtained from digitized pore space images but for the local percolation probability, they used an *ad hoc ansatz* with an adjustable parameter that was varied to obtain good agreement with experimental data.
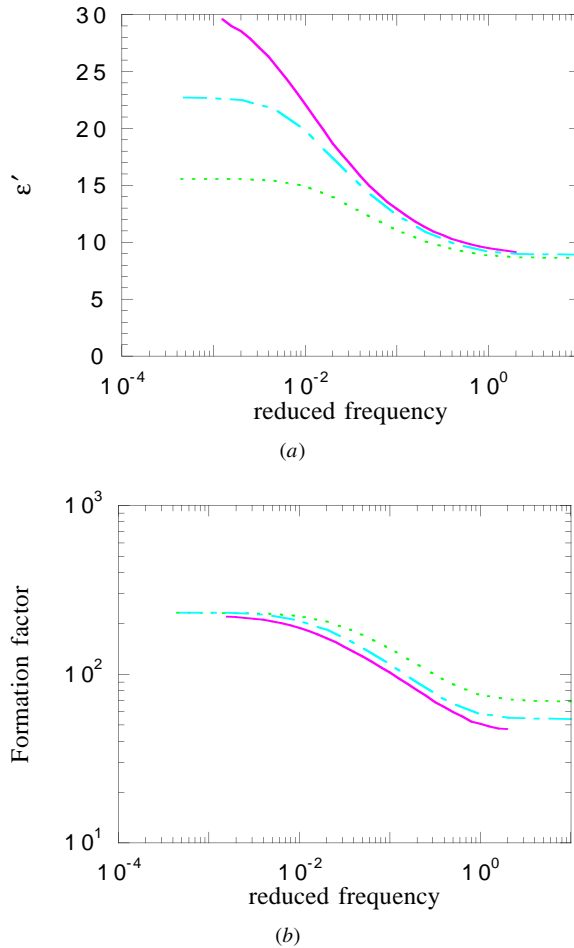
Figure 2. The permittivity (*a*) and the formation factor (*b*) for a sample having 5.2% porosity as measured by Holwech and Nøst (solid line), calculated assuming an initial b.c.c. lattice according to equation (8) (dotted line) and according to equation (11) (chain line).

3. Calculation procedures

According to Holwech and Nøst [9] their unconsolidated packs of unsintered glass spheres had 39% porosity. That is not far from the value of 32%, which applies to a body-centred cubic (b.c.c.) lattice of touching spheres. For simplicity, we chose to use such a lattice as
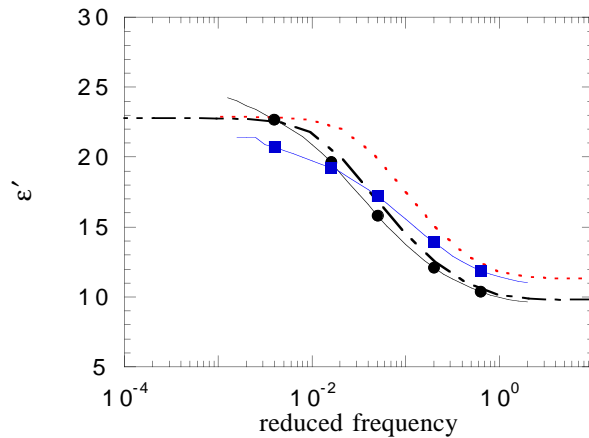
Figure 3. The permittivity as measured by Holwech and Nøst for a sample of 7.3% porosity (solid line, circles) and a sample of 10.7% porosity (solid line, squares) and the predictions obtained using a b.c.c. lattice and equation (11) for 7.3% porosity (chain line) and for 10.7% porosity (dotted line).

a starting point, since the calculations of the dielectric properties of such a lattice can be easily performed. We have performed such calculations using the grain consolidation model (GCM) [21].

We assumed the value of the dielectric constant of water to be 80, and of the glass spheres to be 7 (that choice was motivated by an extrapolation of the high-frequency data of Holwech and Nøst [9] for the dielectric constant to zero porosity). We assumed the conductivity of the water to be 10 mS m^{-1} (since the data are presented as a function of the reduced frequency, ω_w, defined as $\omega_w = \omega \varepsilon_0 \varepsilon'_f / \sigma_f$, where ε_0 is the permittivity of vacuum and ε'_f is the relative permittivity of the fluid, this does not really matter) and that the glass was nonconducting. The results of the GCM calculations are shown in figure 1, where we compare the results with the corresponding outcome from simple cubic (s.c.) and face-centred cubic (f.c.c.) lattices.

The ensuing effective-medium calculations were carried out both according to equation (8), assuming aligned ellipsoids, as well as according to equation (11), assuming randomly oriented ellipsoids. For equation (8), the value of the cementation exponent, m, that Holwech and Nøst found to be 2.2, suffices for determining the parameter A_k and thus for performing the calculations. When we use equation (11), equations (12) and the measured cementation exponent suffice for determining two of the depolarization coefficients, A_k, if the third one is given. As we will show later, the value of this third depolarization coefficient does not influence the results very much. We chose to use the values $A_3 = 0.1$ (yielding $A_1 = 0.77$, $A_2 = 0.13$) and $A_3 = 0.2$ ($A_1 = 0.77$, $A_2 = 0.03$) in the calculations; the first combination was preferred and used in most of our calculations.

4. Results and discussion

The real part of the permittivity is usually frequency dependent. The imaginary part, multiplied by $\omega \varepsilon_0$, yields the frequency-dependent AC conductivity, σ_{AC}. Accordingly, we can define a frequency-dependent formation factor by σ_f / σ_{AC}. In figure 2, we show the frequency dependence of the real permittivity and of the formation factor for a porosity
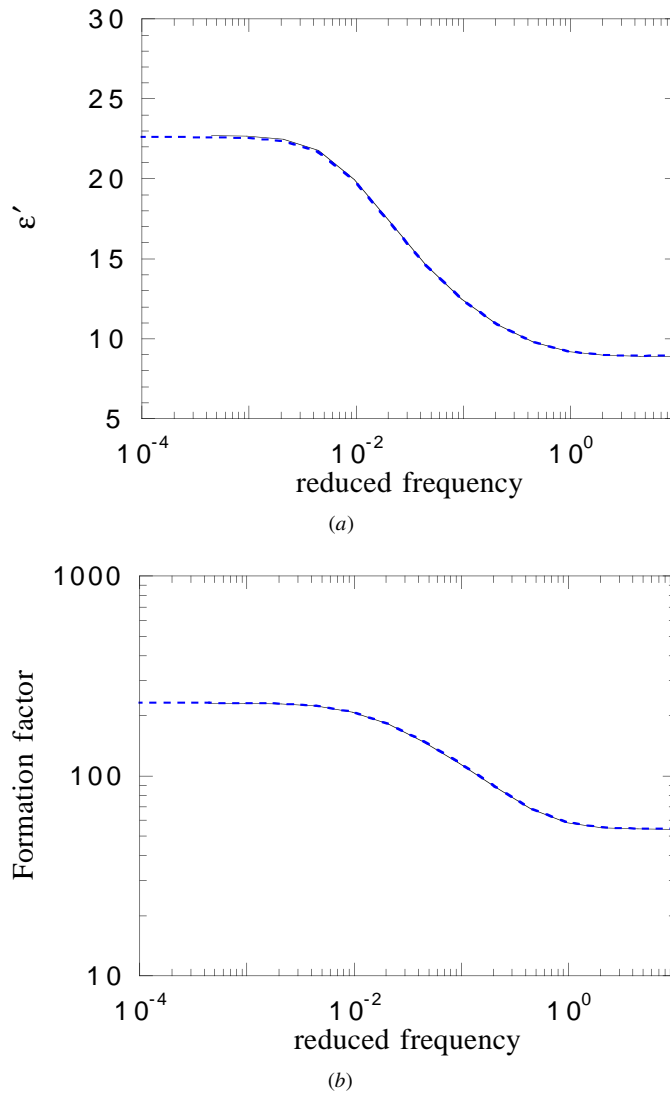
Figure 4. A comparison between the predictions obtained using a b.c.c. lattice and equation (11) assuming $A_3 = 0.10$ (solid line) and $A_3 = 0.20$ (dotted line). The permittivity is shown in (*a*) and the formation factor in (*b*).

of 5.2%, calculated according to equation (8) and according to (11), in both cases using a b.c.c. lattice as a starting point. The data are compared with the results of Holwech and Nøst. For the formation factor, both calculations show fair agreement with experimental results, but the results from calculations according to equation (11) clearly show better agreement. This should not be surprising, since it is clearly not reasonable to assume that the grains form aligned ellipsoids (for an example of the structure of sintered materials see figure 4 in [10]). For the permittivity, equation (11) shows better agreement with experiments than equation (8). Discrepancies arise at the lowest frequencies ($\omega_w < 0.01$), while the agreement for higher frequencies is striking. For the porosity 7.3%, the agreement is even better, as is seen in figure 3, while the agreement for higher porosities is not so good. This we attribute

to the fact that our initial conditions (a regular lattice of 32% porosity) are not the same as the real conditions (a random packing of 39% porosity). In figure 4, we compare the permittivity and the formation factor calculated according to equation (11), using $A_3 = 0.10$ and using $A_3 = 0.20$. The differences are negligible, suggesting that the Archie exponent is sufficient for determining the dielectric properties of the material.
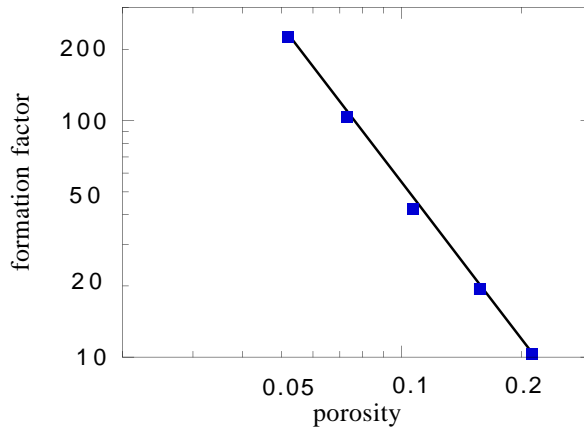

Figure 5. The (low-frequency) formation factor as a function of porosity as measured by Holwech and Nøst (squares) and predicted using a b.c.c. lattice and equation (11) (solid line).

In figure 5, we give the low-frequency formation factor as a function of porosity according to our calculations and according to Holwech and Nøst. It is seen that the agreement is good. In figure 6, we show the predicted porosity dependence of the high-frequency value of ε', ε'_∞, and the high-frequency formation factor, F_∞. The plots have logarithmic scales on both axes and we have subtracted a zero-porosity value of 7.0 from ε'_∞. The results can be very well fitted to power laws, where the exponents in both cases are close to 1.1. However, the fits are not perfect, and it appears—especially for the formation factor—as if the dependence of the porosity is somewhat stronger at higher porosities. Apparently, the power-law behaviour is only an approximation. Note also that the agreement with experimental results (figures 6 and 8 in [9]) for ε'_∞ and F_∞ is good.

One characteristic feature in the experimental results of Holwech and Nøst was the increase in the low-frequency ε' with decreasing porosity. Our calculations yield a low-frequency value of ε' that is fairly independent of porosity, but weakly decreasing with decreasing porosity. It is possible, though, to obtain the reverse porosity dependence, depending on the lattice used and on the value of m, but in such cases the dependence is still very weak.

This discrepancy in the low-frequency permittivity is probably due to the fact that our model does not take into account percolation effects. (The way differential effective-medium theories are constructed, the 'host' material remains continuous down to zero porosity.) The experimental rise in ε' towards low porosities is characteristic of the approach to the percolation threshold [22].

We have also performed calculations for the experiments described by Nøst *et al* in [10]. Here, the exponent m in equation (1) is 2.5, and the depolarization coefficients have to be altered accordingly. Also in this case, we have obtained good agreement between calculations and experiments, except for at low frequencies (reduced frequency below 0.01) at the lowest porosities. In order to improve the DEM theory further, a percolation
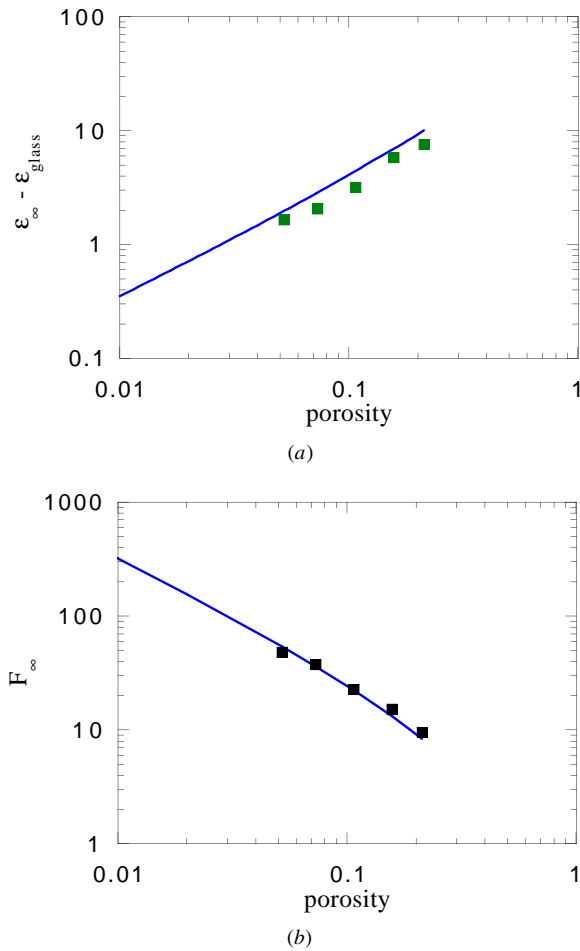
Figure 6. The high-frequency values of the permittivity (*a*) and the formation factor (*b*) as functions of porosity, calculated according to equation (11) (solid lines). The experimental data from Nøst *et al* are shown as squares.

contribution with a depolarization factor $L = 0$ should be included. This would, however, introduce an unknown fitting parameter into the theory. The depolarization factors occurring in our model should not be taken to imply a spheroidal shape of the glass beads. They are instead effective depolarization factors describing dipolar interactions in the sintered sample. It is interesting that Granqvist and Hunderi [23] using results of Clippe *et al* [24] found that the depolarization factors for an f.c.c. lattice of touching spheres are 0.0865, 0.0865 and 0.827. These are not far from the values that we have used and this indicates that our depolarization factors are realistic for lattice-based systems. In our opinion, percolation effects are not included in the calculations of [23, 24].

It should be noted that the local porosity theory of Hilfer [19] is more exact—if it were possible to derive all parameters from images of the sample. Still, our comparatively simple theory manages to yield a satisfactory agreement with experimental data.

5. Conclusions

We have found that the differential effective-medium theory, with a lattice of solid spheres in pore fluid as a starting point, can explain the dielectric spectrum of brine-impregnated samples consisting of sintered glass beads. The main discrepancy is in the prediction for the real part of the dielectric constant at low frequencies. We attribute this discrepancy to the neglect of percolation effects in our model. We have also found that better agreement is obtained when it is assumed that the solid particles are randomly oriented than when it is assumed that they are aligned. Effective depolarization factors describe the interactions between the solid particles.

Acknowledgments

References

[1] Poley J P, Nooteboom J J and de Waal P J 1978 *Log. Analyst* **19** 8–30
[2] Camp P R and Bilotta S 1989 *J. Appl. Phys.* **66** 6007–13
[3] Nettelblad B 1996 *J. Appl. Phys.* **79** at press
[4] Sheng P 1990 *Phys. Rev.* B **41** 4507–12
[5] Sheng P 1991 *Geophysics* **56** 1236–43
[6] Schwartz L M 1994 *Physica* A **207** 131–6
[7] Archie G E 1942 *Trans. Am. Inst. Mining Metall. Eng.* **146** 54–62
[8] Wong P-Z, Koplik J and Tomanic J P 1984 *Phys. Rev.* B **30** 6606–14
[9] Holwech I and Nøst B 1989 *Phys. Rev.* B **39** 12 845–52
[10] Nøst B, Hansen B D and Haslund E 1992 *Phys. Scr.* T **44** 67–70
[11] Brouers F and Ramsamugh A 1986 *Solid State Commun.* **60** 951–3
[12] Maxwell Garnett J C 1904 *Phil. Trans. R. Soc.* A **203** 385–420
[13] Bruggeman D A G 1935 *Ann. Phys., Lpz.* **24** 636–79
[14] van Beek L K H 1967 *Progress in Dielectrics* vol 7, ed J B Birks (London: Heywood) pp 69–114
[15] Bánhegyi G 1986 *Colloid Polym. Sci.* **264** 1030–50
[16] Boned C and Peyrelasse J 1983 *Colloid Polym. Sci.* **261** 600–12
[17] Bergman D J 1978 *Phys. Rep.* **43** 377–407
[18] Milton G W 1981 *J. Appl. Phys.* **52** 5286–93
[19] Hilfer R 1991 *Phys. Rev.* B **44** 60–75
[20] Haslund E, Hansen B D, Hilfer R and Nøst B 1994 *J. Appl. Phys.* **76** 5473–80
[21] Shen L C, Liu C, Korringa J and Dunn K J 1990 *J. Appl. Phys.* **67** 7071–81
[22] Stroud D and Bergman D J 1982 *Phys. Rev.* B **25** 2061–4
[23] Granqvist C G and Hunderi O 1977 *Phys. Rev.* B **16** 3513–34
[24] Clippe P, Evrard R and Lucas A A 1976 *Phys. Rev.* B **14** 1715–21